GATES AND CRELLIN LABORATORIES OF CHEMISTRY

ELECTRON DIFFRACTION INVESTIGATIONS

of the

MOLECULAR STRUCTURES OF CERTAIN COMPOUNDS OF BORON

and of

VOLATILE COMPOUNDS OF THE HEAVY ELEMENTS

by

VERNER SCHOMAKER
Project Supervisor

Technical Report No. 4

July - 1953

Participants in Work: Morton E. Jones, Kenneth Hedberg, Jean A. Hoerni, James A. Ibers, Roy Glauber, Gary Felsenfeld, Richard Marsh, and Verner Schomaker, Project Supervisor.

Contract N6ONR Task Order XXIII
Navy Department
Office of Naval Research

ELECTRON DIFFRACTION INVESTIGATIONS
of the
MOLECULAR STRUCTURES OF CERTAIN COMPOUNDS OF BORON
and of
VOLATILE COMPOUNDS OF THE HEAVY ELEMENTS

1. The Molecular Structures of B_5H_9 and B_4H_{10}

   a. The Structure of Stable Pentaborane. Kenneth Hedberg, Morton E. Jones and Verner Schomaker.
   Reprinted from Proc. Nat. Acad. Sci. U.S., 38, 679 (1952)

   b. On the Structure of Tetraborane. Morton E. Jones, Kenneth Hedberg, and Verner Schomaker.
   Submitted for publication, J. Am. Chem. Soc.

2. Studies of the Theory of Electron Diffraction

   a. Introduction

   b. The Theory of Electron Diffraction. Roy Glauber and Verner Schomaker.
   Reprinted from Phys. Rev., 89, 667 (1953)

   c. Complex Amplitudes for Electron Scattering By Atoms. Jean A. Hoerni and James A. Ibers.
   Accepted for publication, Phys. Rev.

3. X-ray Crystallographic Studies of Beryllium Boride and the Alleged Copper Boride.
   From the thesis of Morton E. Jones, June 1953.

   a. Beryllium Boride

   b. Copper Boride

Technical Report No. 4
July - 1953

Contract N6ONR Task Order XXIII
Navy Department
Office of Naval Research

1. The Molecular Structures of B_5H_9 and B_4H_{10}

   a. The Structure of Stable Pentaborane. Kenneth Hedberg, Morton E. Jones, and Verner Schomaker.
   Reprinted from Proc. Nat. Acad. Sci. U.S., 38, 679 (1952)

   b. On the Structure of Tetraborane. Morton E. Jones, Kenneth Hedberg, and Verner Schomaker.
   Submitted for publication, J. Am. Chem. Soc.

Reprinted from the Proceedings of the National Academy of Sciences
Vol. 38, No. 8, pp. 679-682, August, 1952

THE STRUCTURE OF STABLE PENTABORANE

By Kenneth Hedberg, Morton E. Jones and Verner Schomaker

Gates and Crellin Laboratories of Chemistry,* California Institute of Technology, Pasadena, California

Communicated by Linus Pauling, June 2, 1952

Stable pentaborane, B_5H_9, is one of the boron hydrides, a short, comparatively little studied series of extraordinary compounds for which a satisfactory elementary valence theory is lacking. In 1947 we decided to undertake new electron diffraction studies of the molecular structures. The early diffraction work and most of the theoretical discussion had been too much influenced (it now seems) by unfortunate analogies to ordinary valence compounds, and it had become reasonably clear that at least the old, ethane-like structure for diborane was incorrect and that a bridge structure (I) was more likely. In the case of B_5H_9, also, the structure from

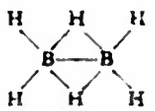

(I)

the previous diffraction study[1] was not in complete agreement with the appearance of the photographs, one of which was available to us. The bridge structure of diborane has now been well established,[2] the crystal structure of decaborane ($B_{10}H_{14}$) has been determined,[3] and the B_5H_9 structure has been determined, both from the gas diffraction pattern in the work here to be described[4] and from an x-ray study of the crystal by Dulmage and Lipscomb.[5] The most impressive attempt at a theory of the compositions and structures, however—Pitzer's protonated double bond theory,[6] which based the structures of all the boron hydrides on diborane bridges and on some plausibly assumed conjugation properties of these bridges—has been a casualty: each of the new boron hydride structures has shown little over-all relation to the previous ones and neither involves the diborane bridge.

The Structure Determination.—The method used has been outlined in recent reports from this laboratory.[7]

New photographs were taken with samples kindly provided by Professor H. I. Schlesinger of the University of Chicago and by Doctor I. Shapiro of the Naval Ordnance Test Station, Pasadena. The camera distance was 10.94 cm. and the electron wave-length 0.0008 Å. Independent visual interpretations of the photographs were made by two observers (see Fig. 1).

The radial distribution curves, showing only two strong peaks, at 1.74 Å. (B—B) and 2.57 Å. (B···B and B···H), exclude both the structure advocated in the original study[1] (II) and that proposed by Pitzer[6] (III):

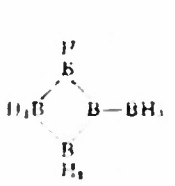

(II)

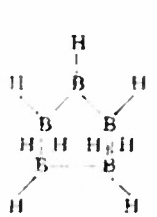

(III)

II would require significant B···B interactions at $1.74\sqrt{2} = 2.46$ Å. and at $2 \times 1.74 \sin 135° / 2 = 3.22$ Å., at least if it were normally rigid, and III at an average of $2 \times 1.74 \sin 108° / 2 = 2.82$ Å. (The original specification of III would also require the 1.74 Å. peak to be obviously doubled.) The radial distribution curves did not lead directly to the structure, mainly because neither the relative areas of the widely separated main peaks nor the indicated absence of minor interactions outside them could be relied upon.

Nevertheless, the radial distribution information provided a starting point for a more detailed analysis of the visual curves themselves. This analysis first showed that the observed doubled character of maximum 9–10 requires two groups of B—B interactions, of about equal weight, separated by 0.11 ± 0.01 Å. Even then, the outer part of the observed intensity curve, including max. 9–10, could not be reproduced without severely restricting the distribution of weights and distances within the 2.57 Å. radial distribution peak, either by making the distribution essentially continuous (corresponding to severe "temperature" factors) or in other ways which, given the B—B split, were fairly obvious. Finally, when this was done on the assumption that the 2.57 Å. peak was due mainly to rigid B···B interactions, it appeared that the B—H terms were probably also split, by about 0.15 Å. into two groups of about equal weight. Corresponding to this distance information three unsymmetrical arrangements of the boron atoms, a puckered five-membered ring, a dimethylcyclopropane-like arrangement, and an ethylcyclopropane-like arrangement, all actually rather closely similar, were found.

Before constructing and testing actual models based on these arrangements of boron atoms (the theoretical intensity curves already calculated lacked the B···H terms), we decided to re-examine the tetragonal pyramid arrangement, which had been considered but rejected in the original diffraction study, had more recently been further advocated by Pauling,[8] and, unlike our unsymmetrical arrangements, was in agreement with recent indications of high symmetry from spectroscopic[9] and calorimetric[10] data. The 2.57 Å. peak now had to be attributed mainly to B···H rather than B···B interactions, contrary to our previous assumption,[11] but with the help of the previous analysis a suitable disposition of hydrogen atoms was readily found (Fig. 2) and all others of full symmetry (C_{4v}) were ten-

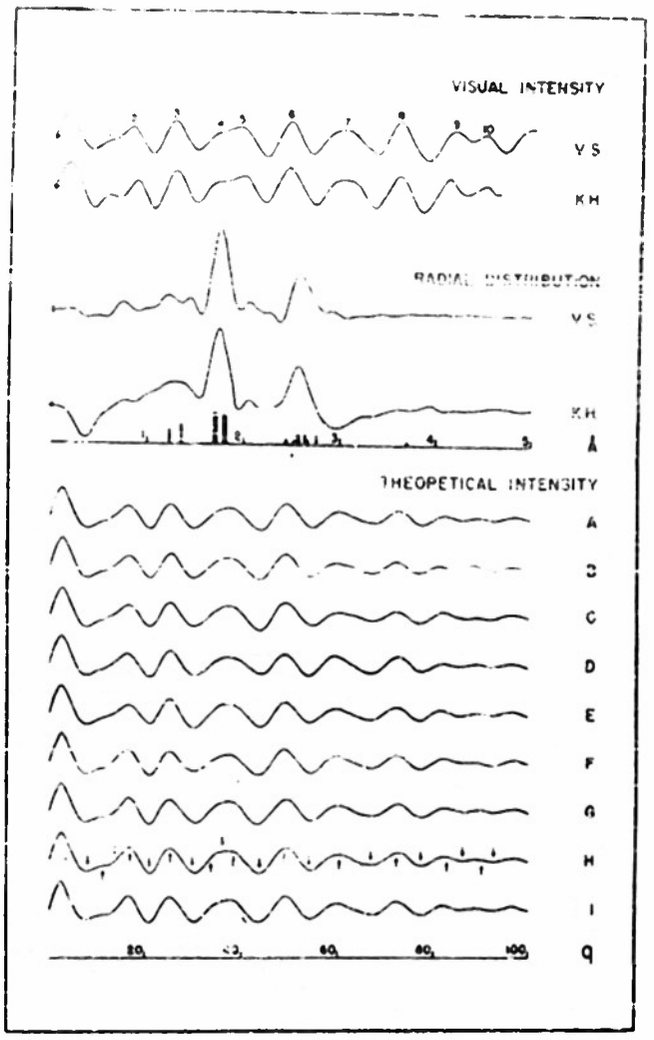

FIGURE 1.

Electron diffraction curves. The theoretical intensity curves are for the following pyramidal models:

Curves	B—Hax./B—Bav.	B—B split	B—H split	$\angle B_1B_2B_3$	external dihedra $\angle B_1B_2B_3$-$B_1B_4H_5$
A	1.275/1.740	0.150	0.150	90°	180°
B	1.275/1.745	0.110	0.150	90°	180°
C	1.275/1.740	0.100	0.050	90°	180°
D	1.275/1.740	0.100	0.250	90°	180°
E	1.225/1.740	0.100	0.150	90°	180°
F	1.325/1.740	0.100	0.150	90°	180°
G	1.275/1.740	0.100	0.150	115°	180°
H	1.275/1.740	0.100	0.150	115°	190°
I	1.275/1.740	0.100	0.150	125°	190°

tatively eliminated. The new structure, with the B_2—B_2 and B_2—H_2 distances the longer of their respective kinds, seemed plausible and met with immediate success.

All except B···H terms were included for the theoretical intensity curves. The coefficients a_i of s^2 temperature factors $\exp(-a_i s^2)$ were taken as 0.00016 for B_2—H_2 and B_1—H_1, 0.00025 for B_2—H_1, 0.00060 for B···H, and zero otherwise, as for diborane,[8] and the effective value 1.25 was used for Z_H. Of the selection of curves shown in Fig. 1, *G*, *H*, and *I* are acceptable, *A*, *B*, and *C* are doubtful, and *D*, *E*, and *F* are unacceptable. Important items for these conclusions are the depth of min. 4, the shape of doublet 4-5, the relative intensities of minima 6, 7, 8, and 9, the shape of max. 7-min. 8, and the position and shape of doublet 9-10. For the best curves, the only point of substantial disagreement concerns the heights of the first three main maxima; it is almost inconsequential for the parameter determination and probably arises from an underestimate, such as could be expected, of the height of the broad inner max. 1-2.

In terms of $B\cdots B_{av.} = 1.740$ Å. the best shape parameter values and estimated limits of error, together with the ranges for which intensity curves were calculated, are: $B\cdots H_{av.}$, 1.288 ± 0.044 Å. (1.22–1.35 Å.); $B\cdots H_{split}$, 0.125 ± 0.090 Å. (0.05–0.35 Å.); $B\cdots B_{split}$, 0.105 ± 0.010 Å. (0.09–0.12 Å.); ∠ $B_1\cdots B_3\cdots H_3$, 120 ± 20° (85–125°); and external dihedral angle $B_1B_2B_3$-$B_4B_5H_5$, 187 ± 10° (165–200°), all for the assumed C_{4v} symmetry. These values and the values of $\langle q_{calc.}/q_{obs.}\rangle_{av.}$ (see table 1 for an example) lead to the following results for the bond lengths: B_1—B_3, 1.700 ± 0.017 Å.; B_2—B_3, 1.805 ± 0.014 Å.; B_1—H_1 and B_5—H_5, 1.234 ± 0.066 Å. (B_1—H_1 = B_5—H_5 assumed); and B_5—H_3, 1.359 ± 0.077 Å.

The limits of error are conservative except that no allowance has been made for the possible effects on the angle determinations of our rough assumption that the previous guess for $a_{B\cdots H}$ in diborane should apply to B_5H_9, for all the different B···H terms. The concentration of all the B···H distances within the 2.57 Å. peak makes the question of interaction between temperature factor and distance parameters more serious than usual, but the boron parameters and probably the B—H distances should not be much affected, since they are determined largely by the outer part of the pattern, where the B···H contribution is in any case small. It may be noted that the crystal[9] and gas values for the bond angles and bond lengths in B_5H_9 are in good agreement except for the B—B lengths, for which the crystal values (1.66 ± 0.02 Å. and 1.77 ± 0.02 Å.) are shorter than ours by possibly significant amounts compared to the limits of error. Our B—B lengths, however, are in good agreement with the preliminary results 1.69 Å. and 1.80 Å. of a recent microwave investigation,[12] from which none of the other parameter values have yet been reported.

The x-ray confirmation of the structure type, which was communicated to us during our parameter determination, made unnecessary any further study of other possibilities, including the unsymmetrical ones described above. The high over-all symmetry and especially the C_{4v} skeletal symmetry have also been confirmed by the microwave investigation.[12]

Discussion.—The B_5H_9 structure has high ligancies, two for the bridge hydrogen atoms, five for the apical boron atom, and six for the basal boron

atoms, in agreement with the principle[13] that electron deficiency gives rise to structures showing ligancies in excess of the respective numbers of suitable atomic orbitals. For the count of ligands, we take the direct B—B interaction of a bridge bond as bonding, although the related B···B interaction in diborane is often regarded as not bonding. We believe our assumption is the more likely one in view of the comparatively short B—B distance. It also makes the ligancies of hydrogen and boron in the boron hydrides and other high-ligancy compounds of boron more uniformly consistent with the high-ligancy principle, and is the natural assumption to make if these compounds are to be related to ordinary covalent compounds in terms of resonance, following Pauling's discussion of the metals.[14] Pauling's relation $r_n = r_1 - 0.300 \log_{10} n$ yields an attractive correlation of the actually very widely varying bond distances,[15] as well as inferences about certain other aspects of the structures. For example, the boron radius which would be exactly compatible with the bond distances of our preliminary report for B_9H_9 is 0.795 Å., in excellent agreement with the average 0.794 Å. obtained from all these compounds.

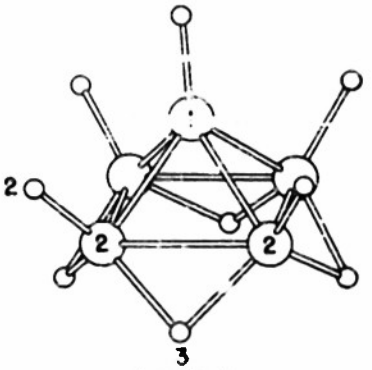

FIGURE 2.
The B_9H_9 structure.

The basal boron atoms of B_9H_9 and the apical boron atoms of $B_{10}H_{14}$ form just the same set of bonds; similarly, the apical boron atoms of B_9H_9 resemble the boron atoms of the calcium boride structure in an octahedron arrangement except for replacement of external B by H. As King and Lipscomb pointed out,[16] moreover, the whole B_9H_9 structure is related to the calcium boride structure in almost precisely the same way as the $B_{10}H_{14}$ structure is related to the boron carbide structure.[17] We may add that the basal boron atoms of B_9H_9 and all the boron atoms of decaborane, as well as the boron atoms of boron carbide and the icosahedron atoms of elementary boron (in the modification of known structure[18]), all have six ligands in the icosahedron arrangement, with bond angles approximating the ideal values of 60°, 108°, and 121$^1/_4$° about as well as would seem possible under the constraints imposed by differing bond lengths and incompatible over-all symmetries.[19] Accordingly, it seems reasonable to suggest that these structures all reflect a strong tendency for sexiligated boron to adopt approximately the ideal icosahedron arrangement.

The occurrence of the icosahedron and octahedron arrangements is remarkable because they are notably anisotropic, in violation of what might be expected to result from the sp^3 (and sp^4, for the hydrides) hybrid

orbitals on which the bonding is presumably mainly based and because there is surely no lack of more conventional alternatives. For elementary boron, for example, ordinary octahedral coordination in the simple cubic structure would seem suitable, especially in view of its frequent occurrence in complex structures for other atoms which are regarded as forming six half-bonds.[20] To be sure, the icosahedron and octahedron arrangements would seem less anisotropic if the external bonds were stronger than the internal bonds, as indeed is the general indication for B_5H_9 and decaborane. For the basal boron atoms of B_5H_9, for example, the bridge B—H, bridge B—B, and slant B—B bonds have the respective Pauling bond numbers 0.45, 0.45, and 0.67, with a total of 2.49, or only about three times the bond number 0.77 of the B—H external bond.[12] But for boron carbide, ele-

TABLE 1

COMPARISONS OF OBSERVED AND CALCULATED POSITIONS OF MAXIMA AND MINIMA FOR MODEL II

	d(Å)				d(calc.)/d(obs.)			
	V. S.		K. H.		V. S.		K. H.	
NO.	MAX.	MIN.	MAX.	MIN.	MAX.	MIN	MAX.	MIN.
1	11.19	7.76	10.89	8.06	(0.956)	(0.979)	(0.983)	(0.943)
2	16.41	13.31	17.31	13.88	(1.012)	(0.939)	(0.959)	(0.901)
3	25.00	20.47	25.34	21.03	1.012	1.021	0.998	0.994
4	33.87	29.70	33.33	29.77	(1.025)	1.024	(1.041)	1.021
5	38.52	35.41	39.66	38.42	(0.971)	(1.011)	(0.943)	(0.983)
6	48.70	43.46	48.59	43.62	1.008	0.999	1.011	0.995
7	59.51	53.53	60.15	54.25	1.000	1.014	0.991	1.007
8	72.66	66.95	71.87	66.61	0.998	1.004	1.009	1.009
9	83.29	78.03	82.23	76.50	(0.984)	0.993	(0.997)	1.013
10	90.07	86.50	89.97	85.57	(0.989)	0.991	(0.991)	1.002
11	..	93.23	..	91.89	...	0.992	...	1.007
			Average, 12 features		1.0047		1.0048	
			Average deviation		0.009		0.007	

mentary boron, and calcium boride there is no definite indication one way or the other. Altogether, a proper understanding of the details of the bonding is lacking.

Nevertheless, it seems unlikely that the immediate bond arrangement in these structures is superior. Instead, the essential point may be that they allow an increase in ligancy without a corresponding increase (or even with a decrease) in the number and severity of close non-bond interactions: compare, for example, the joined icosahedron unit of the boron and boron carbide structures with the simple cubic structure. In the latter, each atom has twelve next-nearest neighbors related to it by 90° bond angles, whereas the icosahedron atom has only five internal next-nearest neighbors at 108° and five external next-nearest neighbors at 122°. This strongly suggests that the next-nearest interactions are repulsive and important

and that the high-ligancy principle should be revised to say that the high ligancies tend to be achieved in such a way as to minimize the numbers and maximize the distances of next-nearest neighbors, even if the resulting bond arrangements would appear by standards of ordinary covalence to be unduly strained. It may also account for the lack of apparent extra strength of the external bonds where two octahedra or two icosahedra are joined: for the icosahedron, again, each external bond would be opposed principally by ten next-nearest interactions at 122° and ten second-nearest interactions (assuming the staggered orientation of groups about the external bond) of the type

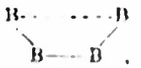

whereas each internal bond is opposed (a full counting shows) by only one internal next-nearest interaction at 108°, two external next-nearest interactions at 122°, and one external interaction of the type

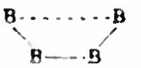

in the opposed orientation. The present situation is evidently related to the cases of cyclopropane and cyclobutane,[21] where the energy and C—C bond length in cyclobutane are both greater than normal, apparently because of cross-ring repulsion, while in cyclopropane, in which the repulsion is avoided by formation of the three-membered ring, the bond length is less than normal and the energy still greater than normal, both apparently in consequence of the angle strain. In the high-ligancy boron compounds the relationships are no doubt different, especially because of the complicated resonance situation; nevertheless, the importance of next-nearest neighbor repulsions seems to be verified and there is the additional indication that angle-strain shortening of the internal bonds may also occur. For the calcium boride structure, of course, the role of the metal atoms has also to be considered.

We should like to express our thanks to Professor Pauling for his continued helpful interest in the investigation.

* Contribution No. 1711. This work was supported in part by the Office of Naval Research under Contract N6-onr-24423.

[1] Bauer, S. H., and Pauling, L., *J. Am. Chem. Soc.*, **58**, 2403 (1936).

[2] (*a*) Price, W. C., *J. Chem. Phys.*, **16**, 894 (1948); **15**, 614 (1947). (*b*) See also Hedberg, K., and Schomaker, V., *J. Am. Chem. Soc.*, **73**, 1482 (1951).

[3] Kasper, J. S., Lucht, C. M., and Harker, D., *Acta Cryst.*, **3**, 436 (1950).

[4] Hedberg, K., Jones, M. E., and Schomaker, V., *J. Am. Chem. Soc.*, **73**, 3538 (1951).

[5] Dulmage, W. J., and Lipscomb, W. N., *Ibid.*, **73**, 3539 (1951).

[6] Pitzer, K. S., *Ibid.*, **67**, 1126 (1945).

[7] See Hedberg, K., and Stosick, A. J., *Ibid.*, **74**, 954 (1952).

[8] Private communication.

[9] Pitzer, K. S., and Pimentel, G. C., private communication.

[10] Taylor, W. J., Beckett, C. W., Tung, J. Y., Holder, R. B., and Johnston, H. L., *Phys. Rev.*, **79**, 234 (1950).

[11] We had at first rejected the tetragonal pyramid (see reference 4), mainly because its relative number of B···B interactions and relative B···B distance ($1.74\sqrt{2} = 2.46$ Å.) are in disagreement with this false interpretation of the 2.57 Å. peak and because, in view of this interpretation, little attention was given to the (crucial) disposition of the hydrogen atoms. Our initial failure to recognize the B—B split also contributed to the argument on the apparent B—B—B angle (i.e., the ratio 2.67/1.74). Actually, the half-width of the 1.74 Å. peak is somewhat greater than would be expected from our convergence factor for zero split (although less than for a 0.10 Å. split). We overlooked this, failing to consider how little widening would result from distance splits up to 0.10 Å., especially in the absence of a well-resolved, sharp term to make the slow decline of the split-term contribution obvious in the appearance of the photographs. (In reference 13 the radial distribution distances were misquoted as 1.76 Å. and 2.62 Å.; also, in the discussion of the puckered five-membered ring model, it was not made clear that for the theoretical curve mentioned the hydrogen terms were neither based on an actual model nor complete. The complete curve was no longer promising; the original curve, lacking the B—B split, of course never was a good fit to the outer part of the pattern.)

[12] Hrostowski, H. J., Myers, R. J., and Pimentel, G. C., *J. Chem. Phys.*, **20**, 518 (1952).

[13] Schomaker, V., *J. chim. Phys.*, **46**, 262 (1949).

[14] Pauling, L., *J. Am. Chem. Soc.*, **69**, 542 (1947).

[15] Hedberg, K., *Ibid.*, in publication.

[16] Private communication; see references 4 and 5.

[17] Clark, J. K., and Hoard, J. L., *J. Am. Chem. Soc.*, **65**, 2115 (1943); Zhdanov, G. S., and Sevast'yanov, N. G., *Compt. rend. acad. sci. U. S. S. R.*, **32**, 432 (1941).

[18] Hoard, J. L., Geller, S., and Hughes, R. E., *J. Am. Chem. Soc.*, **73**, 1892 (1951).

[19] Our values for B_4H_8 are $\angle B_1B_3B_2 = 58°$, $\angle B_2B_3H_3 = 48\frac{1}{2}°$, and $\angle H_3B_3H_3 = 113°$; $\angle B_1B_3H_3 = 106°$, $\angle B_3B_2H_3 = 113°$, and $B_3B_2B_3 = 90°$; and $\angle H_3B_3B_3 = 120°$, $\angle H_3B_3B_3 = 134°$, and $\angle H_3B_2H_3 = 108°$. Here the four-membered ring, the differences of B—H (bridge) and B—B bond lengths, and the evident need for large $\angle H_3B_2H_3$ to provide a reasonably long $H_3\cdots H_3$ distance, which we presume to be non-bonding, are obviously serious constraints; nevertheless, the average external angle is 121°, in surprising agreement with the ideal value. Also, our value 120° for $\angle B_3B_2H_3$ approximately equalizes the external angles, and the smaller, crystal value of 118°, which by the quoted ±5° limit of error is considerably more reliable than ours, equalizes the apparent strains very well indeed.

[20] Runcle, R. E., *J. Am. Chem. Soc.*, **69**, 1327 (1947).

[21] Dunitz, J. D., and Schomaker, V., submitted for publication in the *Journal of Chemical Physics*.

On the Structure of Tetraborane

We have reinvestigated gaseous tetraborane by electron diffraction. The butane-like model with tetrahedral bond angles as reported by Bauer[1] is incompatible with our data; values of $\angle$ B-B-B = 90° and $\angle$ B-B-H = 133.5° do bring it into agreement, but the latter angle is out of the question, especially for the 'methylenic' hydrogen atoms. No exhaustive investigation of the butane-like structure was attempted, however, because a structure (Fig. 1) plausibly related to the known boron hydride structures[2] was discovered and shown to be in excellent agreement with the diffraction pattern early in our work[3,4], and has since been established by Nordman and Lipscomb by the crystal structure investigation reported in the following Communication. The atomic arrangement is closely similar to that of the apical groups in decaborane and is comparable to the arrangements in diborane and stable pentaborane.

Approximate values for the numerous parameters of the C_{2v} model are:

B_1-B_2 = 1.85 Å, B_1-B_3 = 1.76 Å,

$B_3 \ldots B_4$ = 2.88 Å, (Dihedral $\angle$ $B_1B_3B_4$-$B_1B_3B_2$ = 124°32')

B_1-H_5 = B_2-H_7 = B_2H_8 = 1.19 Å,

B_3-H_6 = 1.33 Å, B_4-H_6 = 1.43 Å, H_6 in plane of $B_1B_3B_3$,

$\angle$ B_3-B_1-H_5 = 118°20', and $\angle$ $B_{1,3}$-B_2-$H_{7,8}$ = 117°6'.

These values were obtained primarily from the radial distribution curve (Fig. 2); they were refined by a (necessarily incomplete) correlation treatment. The H_3 parameters are highly uncertain, but the B-H distance, 1.19 Å, and the B-B bond distances warrant comparison with the crystal values.

We are indebted to Professor A. B. Burg and Mr. E. S. Kuljian for the samples of tetraborane and to the Office of Naval Research (Contract N6onr 24423) for support during this investigation.

References

1. S. H. Bauer, J.Am.Chem.Soc., 60, 805 (1938).
2. For references and discussion see K. Hedberg, M. E. Jones, and V. Schomaker, Proc. Nat. Acad. Sci. U.S., 38, 679 (1952).
3. Quarterly Progress Report, October 23, 1951, Contract N6onr 24423.
4. A. B. Burg and G. A. Stone, J.Am.Chem.Soc., 75, 228 (1953).

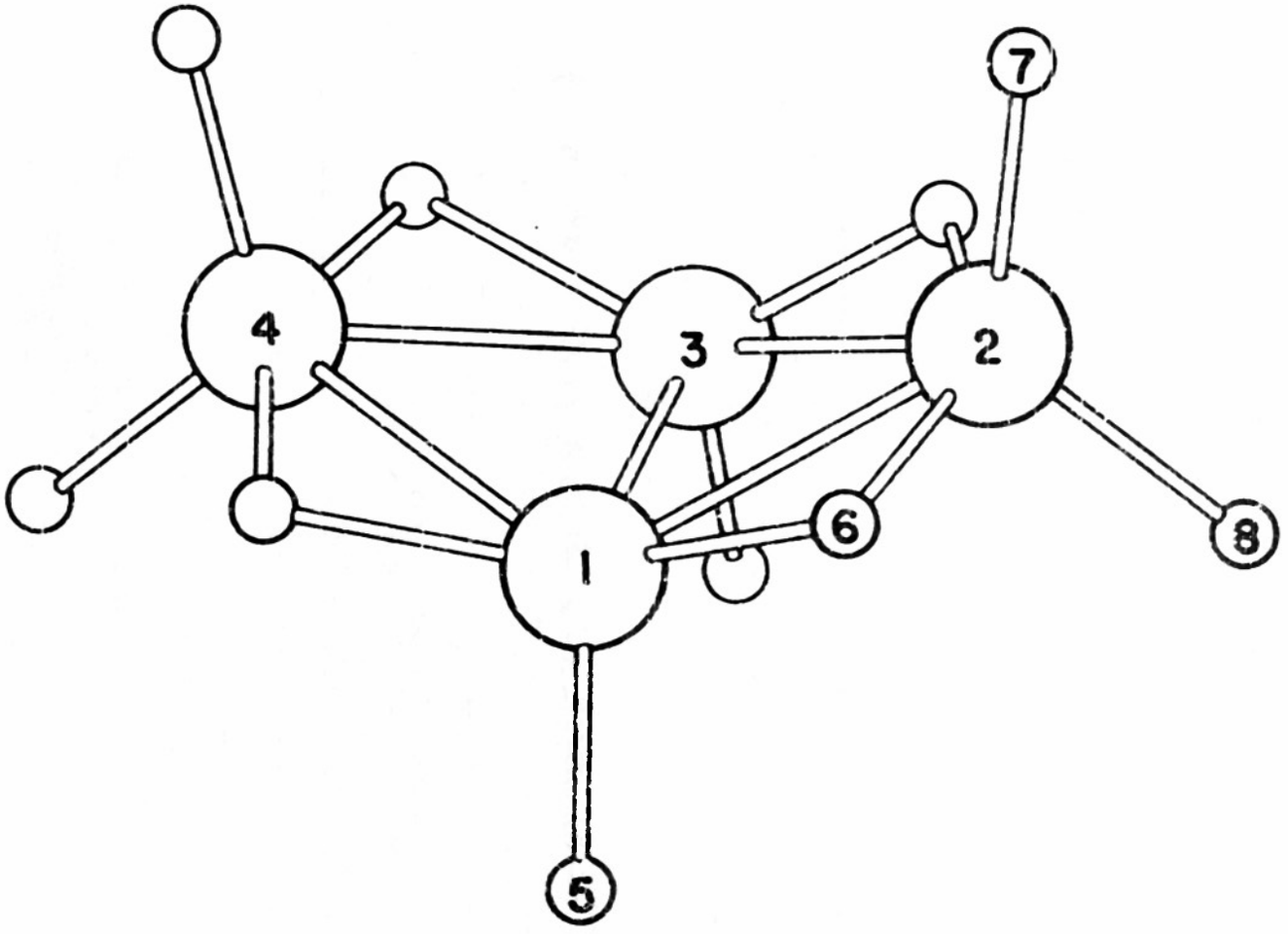

Fig. 1 The B_4H_{10} structure

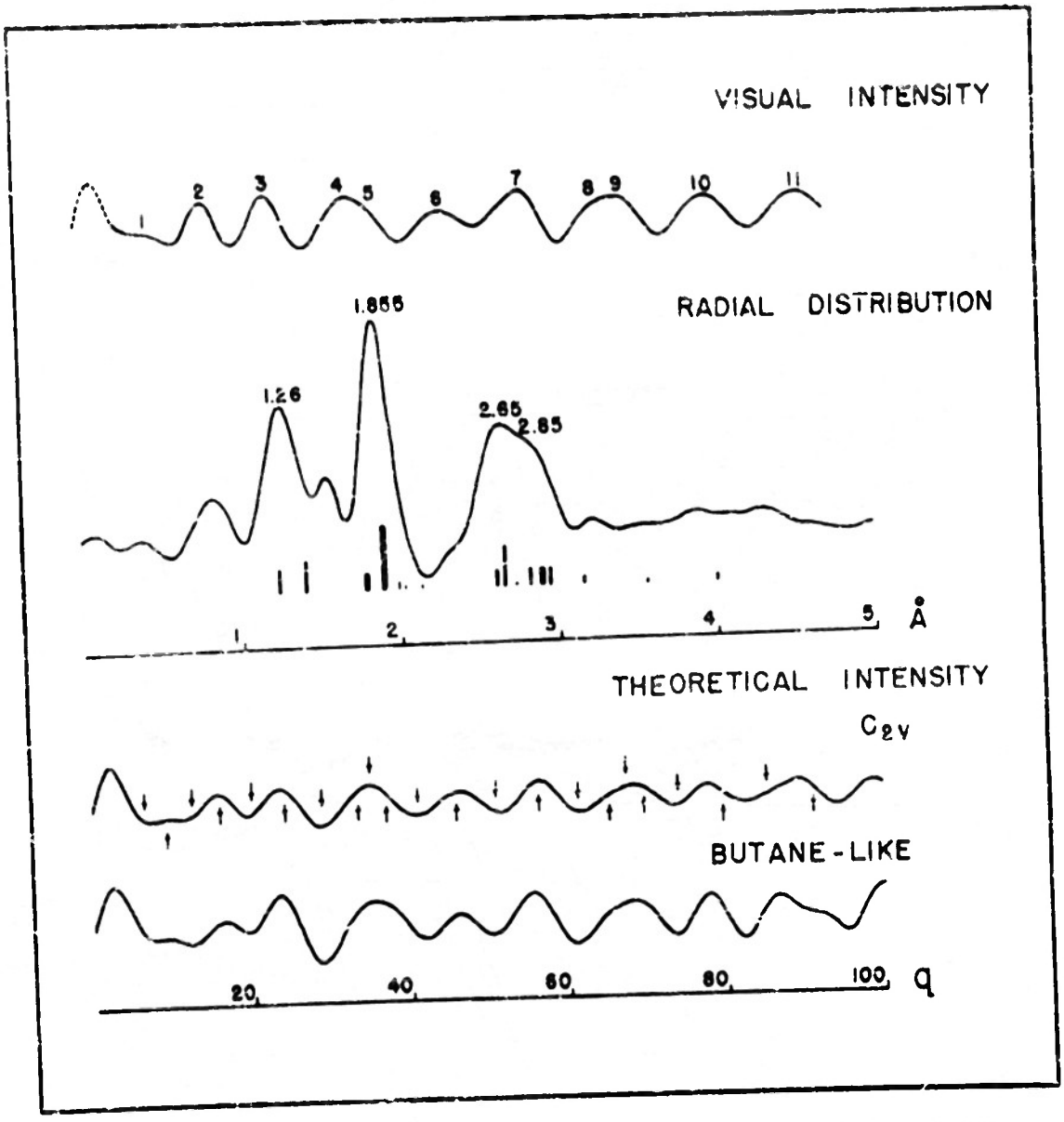

Fig. 2 Visual, radial distribution, and theoretical intensity curves. Theoretical intensity curves are for butane-like model with $\angle$B-B-B = 90° and $\angle$B-B-H = 133.5° and for C_{2v} model described in text.

2. Studies of the Theory of Electron Diffraction

a. Introduction

b. The Theory of Electron Diffraction. Roy Glauber and Verner Schomaker

Reprinted from Phys. Rev., 89, 667 (1953)

c. Complex Amplitudes for Electron Scattering by Atoms. Jean A. Hoerni and James A. Ibers

Accepted for publication in the Physical Review.

Introduction

In our last Technical Report (#3, June 15, 1952) a short account was given of how the unsymmetrical molecular structures that had been derived for a number of compounds of heavy elements are incorrect; how the features of the diffraction patterns that had seemed to demand these unsymmetrical structures are instead a characteristic manifestation of failure of the (first) Born approximation, commonly used in this work; and how satisfactory agreement for symmetrical molecular structures was obtained with a new approximate theory of electron scattering equivalent to the second Born approximation. This account has now been published[1], as has the somewhat longer and more theoretical article which forms the following section of the present report. The technical prospect presented by these articles is of a still attractively simple theory.

Meanwhile, however, the 10 kev UF_6 pattern and the improved calculations mentioned in the second article have shown that both the second Born approximation and the assumption of the screened-Coulomb field, which we have used with it, are inadequate, the uniformly good agreement with the 40 kev experiments apparently representing a quite fortuitous cancellation of the relevant resulting errors. The second following section describes calculations that agree with all the presently available data on UF_6 and are reliable, we believe, both with respect to the atom models and the theoretical treatment of atomic electron scattering which were used. The calculations are lengthy but we hope to extend them sufficiently to provide values of the complex scattering amplitude, $|f(\vartheta)| \exp\{i\eta(\vartheta)\}$, adequate for the usual ($\sim$40 kev) electron diffraction study of any molecule.

Reprinted from THE PHYSICAL REVIEW, Vol. 89, No. 4, 667-671, February 15, 1953
Printed in U. S. A.

The Theory of Electron Diffraction

ROY GLAUBER,* *Norman Bridge Laboratory of Physics, California Institute of Technology, Pasadena, California*
AND
VERNER SCHOMAKER, *Gates and Crellin Laboratories of Chemistry, California Institute of Technology,† Pasadena, California*

(Received October 14, 1952)

It is shown that the omission of an angle-dependent phase factor in the scattering amplitude constitutes a significant error of the Born approximation, as customarily applied to electron diffraction experiments. Some general properties of the scattering amplitude are discussed in relation to the Born approximation and used to derive a simple estimate of the required phase. The theory, thus corrected, is found to remove the need for assuming rather distorted structures in some molecules containing heavy atoms. The effect discussed is present quite generally in the interference of waves scattered by differing potentials and becomes more prominent as the particle energy is lowered. In the Appendix a semiclassical procedure is used to treat the analogous effect in proton diffraction.

THE Born approximation is well known to predict exactly, in the nonrelativistic region, the intensity of electrons scattered by a Coulomb field. Although still a perturbation method, it has seemed in this case nearly immune from the usually attendant inaccuracies and has been widely and successfully used in the analysis of electron diffraction patterns. Confidence in the approximation as ordinarily applied to molecular structure determinations has extended even to a number of cases which have seemed to reveal rather improbable structures. On re-examining several of these (which are briefly noted in Sec. I), we have found that a phase change, heretofore neglected, which takes place on scattering is the probable cause of the anomalies.[1] It may, in extreme cases, lead to strikingly altered conclusions about molecular structure. The error is one characteristic of the Born approximation and appears whenever it is applied to the interference of waves scattered by potentials of different strengths. The phase shift in question, which depends significantly on the effects of screening, is calculated approximately in Sec. II, and the results are then compared with experiment.

I. NATURE OF THE EFFECT

The diffraction patterns of electrons scattered by gases consist of weak concentric rings superposed on the intense forward maximum of Coulomb scattering (modified by screening). Fourier analysis of the ring structure gives the distances between the scattering centers of the molecule. In some molecules containing heavy atoms a curious effect involving these distances has been found. Uranium hexafluoride, in which the effect was first noted, might be expected to show octahedral symmetry about the uranium atom. The molecule has instead appeared rather puzzlingly asymmetric: the calculated curves showing the distribution of interatomic distances[2] have two distinctly separated peaks at 1.87A and 2.17A rather than a single one corresponding to a unique U—F bond length. Information from other sources, however, in no way confirms this picture. The data on infrared spectra, molecular entropy, and the dipole moment are all consistent with the symmetrical structure.[3] Similar apparent asymmetries have also been found to occur in a number of other molecules of the form MX_n, containing single heavy atoms. The distances between the heavy atom and its neighbors are apparently split into two equal groups differing by an amount roughly proportional to $Z_M - Z_X$. For equal atomic numbers as in the heavy molecule I_2, nothing unusual is observed.

We shall not dwell upon the valence-theoretical

* Present address: Lyman Laboratory of Physics, Harvard University, Cambridge 38, Massachusetts.
† Contribution No. 1743.
[1] V. Schomaker and R. Glauber, Nature 170, 290 (1952).
[2] S. H. Bauer, J. Chem. Phys. 18, 27 (1950).
[3] See especially Bigeleisen, Mayer, Stevenson, and Turkevich, J. Chem. Phys. 16, 442 (1948); and Burke, Smith, and Nielsen, J. Chem. Phys. 20, 447 (1952).

attempts which have been made to explain these results. The smoothness of the dependence on nuclear charges indicates an inadequacy of the scattering theory rather than any actual effects of chemical bonding. In demonstrating this we shall show that the molecules in question are in fact as accurately symmetrical as the present diffraction techniques may discern.

Of the various inaccuracies implicit in the conventional calculations, the most obvious, perhaps, is the use of the Born approximation for the atomic scattering amplitudes. Other points more specifically molecular in nature are the neglect of multiple scattering (by the different atoms) and of valence distortion of the charge distribution. A strong dependence on the difference of atomic numbers cannot, however, be produced by either of the latter two effects, whereas interference between corrections to the atomic scattering amplitudes may easily do so. For this reason we assume that the wave scattered by a molecule may still be represented by a superposition of waves $f_j(\mathbf{k}', \mathbf{k})e^{ikr}/r$ scattered by the individual atoms ($j=1, 2, 3, \cdots$) from the direction $\mathbf{k}$ to the direction $\mathbf{k}'$.

The amplitudes $f_j(\mathbf{k}', \mathbf{k})$ may be shown quite generally (see Sec. II) to be complex functions of the scattering angle. It is characteristic of the Born approximation, however, that these amplitudes, given by the familiar matrix element,

$$f_B(\mathbf{k}', \mathbf{k}) = -\frac{m}{2\pi\hbar^2}\int e^{i(\mathbf{k}-\mathbf{k}')\cdot\mathbf{r}}V(\mathbf{r})d\tau, \qquad (1)$$

are always real for atomic scattering potentials $V(\mathbf{r})$ (or more generally, for any potential unchanged by inversion in the origin). An example close at hand is scattering by a pure Coulomb field, for which the expression (1) predicts exactly the absolute value of the scattered amplitude but omits at the same time a phase factor sensitively dependent on the angle of scattering.[4] Abbreviating the amplitudes for the moment, as $f_j(\theta)$, we take explicit account of their phases by writing them as $|f_j(\theta)|\exp(i\eta_j(\theta))$. The intensity of the scattered electrons averaged over the random orientations of the gas molecules is then proportional to

$$\sum_{i,j} f_i^*(\theta)f_j(\theta)\frac{\sin sr_{ij}}{sr_{ij}} = \sum_{i,j}|f_i(\theta)||f_j(\theta)| \times\cos\{\eta_i(\theta)-\eta_j(\theta)\}\frac{\sin sr_{ij}}{sr_{ij}}, \qquad (2)$$

where $s=|\mathbf{k}-\mathbf{k}'|=(4\pi/\lambda)\sin(\theta/2)$, and r_{ij} is the distance between atoms i and j.

To see the way the phase $\eta(\theta)$ may explain the apparent asymmetry, let us suppose the amplitudes $f_j(\theta)$ are real. Then the sum of the terms contributed by a split pair of distances $r_{ij}=r_0-\delta$ and $r_{ij'}=r_0+\delta$ with similar atoms j and j', would be approximately

$$2|f_j(\theta)||f(\theta)|\cos s\delta\sin sr_0/sr_0. \qquad (3)$$

(The amplitude difference, of order δ/r_0, is neglected.)

This expression is of just the form that would be given by (2) if the phase difference $|\eta_i(\theta)-\eta_j(\theta)|$ were proportional to s, and if no distance splittings at all existed. The scattering angle at which the amplitude of the wave corresponding to (3) first changes sign (and vanishes) is given by $|\eta_i(\theta)-\eta_j(\theta)|=\pi/2$. In practice it is the behavior of the diffraction pattern in the neighborhood of this critical angle that has been principally responsible for the interpretation in terms of bearing fine waves and its implied molecular asymmetry. It is hoped that in future experiments the very faint outer fringes of the diffraction pattern may be observed at scattering angles sufficiently large to include the second critical angle $|\eta_i(\theta)-\eta_j(\theta)|=3\pi/2$. Since these data are lacking, the correct prediction of the scattering angle for which the phase difference is $\pi/2$ is the only quantitative test now available.

Moderate deviations of the phase shift from linearity in s on either side of the single critical angle observed will not very noticeably change the character of the predicted pattern. Indeed the desire that $|\eta_i(\theta)-\eta_j(\theta)|$ be linear in s comes from comparison with the asymmetric model, whose fit to the experimental diffraction pattern, although good, is not beyond improvement. The theoretically predicted phase differences (see Sec. II) which are monotonically increasing functions of s (but not proportional to s) appear in fact to fit the observed patterns more satisfactorily than the asymmetric model.[5]

II. THEORY

Before specializing to the atomic case, it will be useful to discuss several quite general properties of scattering amplitudes. Let us suppose $\psi_{\mathbf{k}}(\mathbf{r})$, $\psi_{\mathbf{k}'}(\mathbf{r})$ and $\psi_{-\mathbf{k}'}(\mathbf{r})$ are solutions of the Schrödinger equation for equal energies arising from initial plane waves in the directions $\mathbf{k}$, $\mathbf{k}'$, and $-\mathbf{k}'$, respectively. They then obey the relations

$$\psi_{-\mathbf{k}'}\nabla^2\psi_{\mathbf{k}}-\psi_{\mathbf{k}}\nabla^2\psi_{-\mathbf{k}'}=0, \qquad (4a)$$

$$\psi_{\mathbf{k}'}^*\nabla^2\psi_{\mathbf{k}}-\psi_{\mathbf{k}}\nabla^2\psi_{\mathbf{k}'}^*=0, \qquad (4b)$$

which, integrated over the volume of a sphere surrounding the scatterer, are immediately expressed as the surface integrals

$$\int_S\left(\psi_{-\mathbf{k}'}\frac{\partial}{\partial r}\psi_{\mathbf{k}}-\psi_{\mathbf{k}}\frac{\partial}{\partial r}\psi_{-\mathbf{k}'}\right)dS=0, \qquad (5a)$$

$$\int_S\left(\psi_{\mathbf{k}'}^*\frac{\partial}{\partial r}\psi_{\mathbf{k}}-\psi_{\mathbf{k}}\frac{\partial}{\partial r}\psi_{\mathbf{k}'}^*\right)dS=0, \qquad (5b)$$

[4] For the exact solution see N. F. Mott and H. S. W. Massey, *Theory of Atomic Collisions* (Oxford University Press, London, 1949), second edition, p. 48.

[5] G. Felsenfeld and J. Ibers, private communication.

with dS an element of surface. If the radius of the sphere is made sufficiently large, the wave functions assume their asymptotic values on the surface. We may then substitute

$$\psi_k(r) = \exp(i\mathbf{k}\cdot\mathbf{r}) + f(\mathbf{k}_r, \mathbf{k}) \exp(ikr)/r$$

(where $\mathbf{k}_r$ is a propagation vector in the direction $\mathbf{r}$; $|\mathbf{k}_r| = k$) together with the analogous expressions for the other wave functions. The asymptotic values of the surface integrals for large sphere radii are then easily found and furnish two important relations involving the scattering amplitude. The first of these, coming from (5a), is

$$f(\mathbf{k}', \mathbf{k}) = f(-\mathbf{k}, -\mathbf{k}'), \tag{6}$$

which expresses the reversibility of the scattering between any pair of directions. From (5b) we find the relation

$$\frac{1}{2i}\{f(\mathbf{k}', \mathbf{k}) - f^*(\mathbf{k}, \mathbf{k}')\} = \frac{k}{4\pi}\int f^*(\mathbf{k}'', \mathbf{k}')f(\mathbf{k}'', \mathbf{k})d\Omega_{k''}, \tag{7}$$

in which the vector $\mathbf{k}''$ on the right is integrated over the sphere $|\mathbf{k}''| = k$. For the particular case $\mathbf{k}' = \mathbf{k}$, Eqs. (4b) and (5b) express the conservation of the particle current. Equation (7) then reduces to

$$\mathrm{Im} f(\mathbf{k}, \mathbf{k}) = (k/4\pi)\sigma \tag{8}$$

(where σ is the total scattering cross section), a relation which illustrates how fundamental is the requirement that the amplitude of the scattered wave be complex rather than real.

The more general form of Eq. (7) may be simplified by assuming that the scattering potential has inversion symmetry $V(\mathbf{r}) = V(-\mathbf{r})$. Nothing then is changed by inverting all vectors in the origin, and it follows, in particular, that $f(\mathbf{k}', \mathbf{k}) = f(-\mathbf{k}', -\mathbf{k})$. The latter relation together with the principle of reversibility (6) shows that the scattering amplitude is symmetric:

$$f(\mathbf{k}', \mathbf{k}) = f(\mathbf{k}, \mathbf{k}'). \tag{9}$$

Equation (7), under our assumption, then reduces to

$$\mathrm{Im} f(\mathbf{k}', \mathbf{k}) = \frac{k}{4\pi}\int f^*(\mathbf{k}', \mathbf{k}'')f(\mathbf{k}'', \mathbf{k})d\Omega_{k''}, \tag{10}$$

a relation we shall have frequent occasion to apply.

The reason for the inadequacy of the Born approximation (i.e., the first term of a power series expansion in $\alpha = -Ze^2/\hbar v$) in the present context is easily seen from (10). For $f(\mathbf{k}', \mathbf{k}) = O(\alpha)$ we have $\mathrm{Im} f(\mathbf{k}', \mathbf{k}) = O(\alpha^2)$, from which it follows that the phase increases with α, $\eta(\mathbf{k}', \mathbf{k}) = \arg f(\mathbf{k}', \mathbf{k}) = O(\alpha)$. Clearly then we must either go beyond the first term of the series or employ a fundamentally more accurate formulation of the scattering problem. In the present work we shall use some assumptions based on our experience with Coulomb scattering to simplify the higher terms of the Born series, thereby avoiding a good deal of numerical work but allowing still a reasonable comparison with experiment. We shall leave to a later treatment the refinements introduced by a basically different and more accurate procedure for approximating the scattering amplitude, calculations for which are now in progress.

At the energies at which diffraction experiments are performed (~40 kev), electron wavelengths are substantially smaller than the atomic radius a, ($ka \sim 10$ to 20). For all save small angles ($\theta \sim 1/ka$), therefore, the intensity of scattering is negligibly affected by the screening of atomic fields. For these angles the Rutherford formula and, hence, the Born approximation intensities are nearly exact. At smaller angles the effects of screening are partially accounted for by the structure factor implicit in (1). We shall assume for simplicity that the Born approximation (1) represents the absolute value of the scattering amplitude at all angles. The characteristic features of the simpler diffraction patterns are in any case quite insensitive to the over-all atomic scattering intensities.

The difference between screened and unscreened Coulomb fields becomes particularly important for the phase of the scattering amplitude. For the unscreened field the phase of the exact solution[4] contains principally the coordinate-dependent term $-\alpha \log\{kr(1-\cos\theta)\}$, which increases indefinitely with r, the distance from the scatterer. This is, of course, a property peculiar to the slow decrease of the Coulomb potential and is absent for screened fields. A simple estimate of the phase in the screened case may be obtained by substituting the Born approximation amplitude $f_B(\mathbf{k}', \mathbf{k})$ on the right side of (10) and equating both sides to order α^2. We obtain

$$\eta(\mathbf{k}', \mathbf{k}) = \frac{k}{4\pi f_B(\mathbf{k}', \mathbf{k})}\int f_B(\mathbf{k}', \mathbf{k}'')f_B(\mathbf{k}'', \mathbf{k})d\Omega_{k''}, \tag{11}$$

an expression which is equivalent to the second Born approximation.

To evaluate the phase, we chose as an analytically convenient model of the screened field the exponential form

$$V(r) = -Ze^2e^{-r/a}/r, \tag{12}$$

for which the Born approximation amplitude is

$$f_B(\mathbf{k}', \mathbf{k}) = -2\alpha ka^2/(|\mathbf{k}' - \mathbf{k}|^2a^2 + 1). \tag{13}$$

The angular integration of (11) is not difficult to perform, and the resulting phase, as a function of the scattering angle θ, is

$$\eta(\theta) = -2\alpha\left(1 + \frac{1}{4k^2a^2\sin^2(\theta/2)}\right)A\tanh^{-1}A, \tag{14}$$

with

$$A = \frac{\sin(\theta/2)}{[(1 + (1/2k^2a^2))^2 - \cos^2\theta/2]^{\frac{1}{2}}}. \tag{15}$$

Since $2k^2a^2 \gg 1$ these expressions may be reduced to

$$\eta(\theta) \sim -2\alpha \frac{1+s^2a^2}{sa(4+s^2a^2)^{\frac{1}{2}}} \tanh^{-1}\frac{sa}{(4+s^2a^2)^{\frac{1}{2}}}, \quad (16)$$

in which we have once again used the notation

$$s = |\mathbf{k}' - \mathbf{k}| = 2k \sin(\theta/2).$$

A graph of $|\eta(\theta)/\alpha|$ according to Eq. (16) is given in Fig. 1. For the forward direction, the value $\eta(0) = -\alpha/2$ is quite insensitive to the screening radius. For large angles the phase is asymptotically

$$\eta(\theta) \sim -2\alpha \log(2ka \sin\theta/2), \quad (17)$$

the value of which may in practice be appreciable, even for the lighter elements.

The validity of the expression (16) for the phase, at least for large angles, is somewhat stronger than its derivation by the present perturbation procedure might imply. This may be seen by exploiting the similarity of the large angle scattering by screened and unscreened Coulomb fields.[6] In particular the dependence of the asymptotic phase (17) on θ is the same (apart from an additive constant) as that of the exact Coulomb phase, a fact which implies correctly that for angles $\theta \gg 1/ka$ the scattering amplitudes for the screened and unscreened fields differ only by a phase factor, independent of angle.[7]

In undertaking comparisons with experimental results we shall assume that the estimate of the phase given by (16) is sufficiently accurate to be used directly[8] in

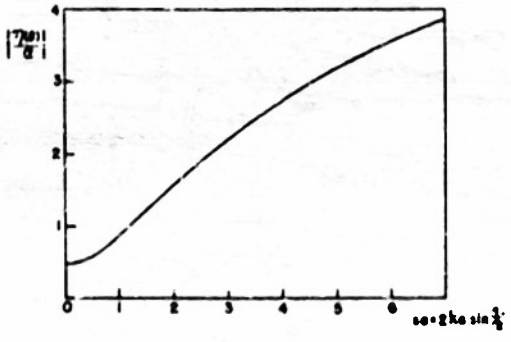

FIG. 1. Graph of the dependence of the phase on scattering angle: $|\eta(\theta)/\alpha|$ *vs* $2ka \sin(\theta/2)$, as given by Eq. (16).

[6] It may also be seen from the work of R. Dalitz [Proc. Roy. Soc. (London) A206, 509 (1951)], who has derived the asymptotic form (17) and shown that its occurrence as a phase is consistent with the third Born approximation as well as the second.

[7] This behavior is implicitly made use of in computing the Coulomb scattering of identical particles when one of them is screened (e.g., p-$\bar{p}$ scattering). The constant phase factor by which the Coulomb and correctly screened solutions differ is not observed. For other potentials the interference effect involved in the scattering of similar particles will also require a knowledge of the angle-dependent part of the phase, omitted in the first Born approximation.

[8] Our procedure here actually goes beyond the second Born approximation, which, strictly speaking, would only consider the terms of (2) to order α^2, and would thereby eliminate the contribution of the phase entirely.

the formalism of Sec. I. The accuracy of this method is difficult to estimate without performing numerically more involved calculations. We may mention, however, that the preliminary results obtained using a more accurate method (based on the smallness of α/ka rather than α) are favorable. They indicate that the accuracy of (16) for $\alpha \sim 1$ is roughly commensurate with that of the screening model (12).

III. COMPARISON WITH EXPERIMENT

While the phase shift we have discussed will modulate the intensities of the diffraction patterns of all heteratomic molecules, its effect is most strongly felt when large differences in the nuclear charges prevail. In such cases the attempt to account in the conventional way for the observed modulation has led, as we have already noted in Sec. I, to the assumption of curiously unsymmetrical molecular structures. For a proper interpretation in the light of the present work, the diffraction data for each of the molecules in question will eventually require detailed re-analysis. A simple way, however, of checking the corrected theory is to show the way in which the treatment based on symmetrical models with phase shifts is able to duplicate the numerical results previously arrived at for the apparent asymmetries. To do this we note by comparing (2) and (3) the approximate relation

$$2\delta = \pi/s_{crit}, \quad (18)$$

in which s_{crit} is the value of $2k \sin(\theta/2)$ for which the phase difference is $\pi/2$. An approximate value of the screening distance, adequate for the calculation is $a = 0.528Z^{-\frac{1}{3}}$A. The predicted apparent "splits" (2δ) that result are listed in Table I along with the corresponding experimental values. Their agreement, it may be seen, is quite close. It follows that for these molecules the diffraction patterns predicted by the present formulation will be in good agreement with those observed. The intensity curve calculated for UF_6 at 40 kev seems to show even better agreement than the previous work for the central and outer parts of the pattern.[4] This is a consequence of the deviation of the phases from proportionality to s.

A large number of electron diffraction studies of molecules containing heavy atoms are on record in which nothing anomalous was observed, a circumstance which no doubt helped delay the recognition of the phase shifts. It is important, therefore, to remark that in all the adequately reported cases, the pattern was observed only at angles at which the phase difference is less than the critical value $\pi/2$.

The phase given by Eq. (16) is increased by lowering the electron energy, and its modulation of the diffraction pattern varies more rapidly with s. The resulting energy dependence of the pattern is a feature absent from any treatment based on the first Born approximation. Some photographs of UF_6, taken at 10 kev do indeed show changes in the direction predicted,[4] and will be analyzed

Complex Amplitudes for Electron Scattering by Atoms*

Jean A. Hoerni and James A. Ibers**

Gates and Crellin Laboratories of Chemistry
California Institute of Technology, Pasadena, California

ABSTRACT

The partial waves scattering theory has been applied to electron scattering by U and F atoms at 40 and 11 kev. The electron scattering by the UF_6 molecule, predicted from these results, is in good agreement with experiment.

I. INTRODUCTION

Recently, Schomaker and Glauber[1] have pointed out that anomalies, e.g. apparent asymmetry, in the structures of molecules containing both heavy and light atoms as determined by electron diffraction can be removed by using complex atomic scattering amplitudes, $f(\theta)$, and hence by rejecting the first Born approximation which gives only real amplitudes. This approximation, although theoretically justified only for $-a = Ze^2/(\hbar v)$ small, has nevertheless been universally employed in investigations of the molecular structure of gases by electron diffraction. Using the second Born approximation, Glauber and Schomaker[2] evaluated the phase of the complex amplitude, $\eta(\theta) = \arg f(\theta)$, for the screened-coulomb field. In this way remarkably good agreement was obtained for a large group of molecules at 40 kev. However, good agreement is not obtained for the

UF_6 pattern at 11 kev,[3] and, in any case, the second Born approximation and the assumption of a screened-coulomb field are both uncertain, so that a more adequate calculation is desired. We describe below the application of the partial waves scattering theory to the problem of the scattering of electrons by atoms (U and F). The energies considered (11 and 40 kev) are sufficiently high so that electron exchange and polarization effects can be neglected.

II. THEORY[4]

The solution to the problem of the elastic scattering of a beam of particles by a central potential $\underline{V}(\underline{r})$ is given by

$$f(\theta) = (2ik)^{-1} \sum_{\ell=0}^{\infty} (2\ell+1)(e^{2i\delta_\ell} - 1) P_\ell(\cos\theta), \qquad (1)$$

where θ is the scattering angle, $\underline{k}$ is $2\pi/\lambda$, and the phases, $\delta_{\underline{\ell}}$, may be interpreted as the phase differences between the perturbed and unperturbed radial functions at large distances from the nucleus. The $\delta_{\underline{\ell}}$'s can be evaluated in several ways for electron scattering. When $\delta_{\underline{\ell}} \ll 1$, (1) can be rewritten as

$$f(\theta) = k^{-1} \sum_{\ell=0}^{\infty} (2\ell+1)\ \delta_\ell P_\ell(\cos\theta) \qquad (2)$$

and the $\delta_{\underline{\ell}}$'s are given by

$$\delta_\ell^{\circ} = \frac{kc}{Ze^2} \int_0^\infty V(r)\, J^2_{\ell+\frac{1}{2}}(kr)\, r\,dr \qquad (3)$$

Substitution of (3) into (2) yields the first Born approximation for the scattering amplitudes, namely

$$f^B(\theta) = \frac{2ka}{Ze^2} \int_0^\infty V(r)\, \frac{\sin(sr)}{sr}\, r^2\, dr, \qquad (4)$$

where $s = 2k \sin(\theta/2)$. When the δ_ℓ's are not small, they may be evaluated conveniently by the WKB method. Starting with the relativistic Schrödinger equation

$$\nabla^2\psi + K^2(r)\psi = 0, \qquad (5)$$

where

$$K^2(r) = \frac{[E-V(r)]^2 - m^2c^4}{\hbar^2c^2} = k^2 + \frac{V^2(r) - 2E\,V(r)}{\hbar^2c^2},$$

we obtain

$$\delta_\ell = \int_{r_1}^{\infty} G(r)\,dr - \int_{r_2}^{\infty} G_0(r)\,dr \qquad (6)$$

with

$$G(r) = \left\{k^2(r) - \left[(\ell+\tfrac{1}{2})/r\right]^2\right\}^{1/2}, \quad G_0(r) = \left\{k^2 - \left[(\ell+\tfrac{1}{2})/r\right]^2\right\}^{1/2}$$

Here, the energy E includes the rest energy, and r_1, $r_2 > 0$ are the zeros of the respective integrands. In accordance with the work of Langer,[5] we have replaced $\ell(\ell+1)$ by $(\ell+\frac{1}{2})^2$. The δ_ℓ's may also be evaluated exactly. This has been done by Bartlett and Welton[6] with a differential analyzer for Hg at 100 and 230 kev starting with Gordon's solutions of the Dirac equation. Although the δ_ℓ's from the WKB method are generally supposed to be reliable only when large, and hence only when ℓ is small, Bartlett and Welton found these values to be in excellent agreement with the exact values over the entire range of ℓ; they found the δ_ℓ's to be reliable at large ℓ.

III. PROCEDURE AND RESULTS

We first compute the complex atomic scattering amplitudes for U and F at 40 and 11 kev and then apply these to the scattering by the UF_6 molecule. UF_6 was selected because it offers the most severe test (the molecule exhibits the largest apparent asymmetry[1]) and because only for it do we have electron diffraction photographs prepared at 11 kev as well as at the usual 40 kev.

For U we adopted the Thomas-Fermi potential, using the approximate form[7]

$$V(r) = -\frac{Ze^2}{r} \sum_{i=1}^{3} a_i e^{-b_i r/a} \qquad (7)$$

where $a_1 = 0.10$, $a_2 = 0.55$, $a_3 = 0.35$, $b_1 = 6.0$, $b_2 = 1.2$, $b_3 = 0.3$, and a, the screening radius, is $0.4685/Z^{1/3}$. For F we used the Hartree potential[8] in the approximate form

$$V(r) = -\frac{Ze^2}{r} (e^{-\beta_1 r} + c\, r\, e^{-\beta_2 r}) \qquad (8)$$

where $\beta_1 = 3.94$, $\beta_2 = 17.0$, and $c = -2.67$. Preliminary calculations indicated that the effect of electron spin would be important only for $l \leq 2$,[9] and since in the final summation (1) these terms are reduced in importance by the factor $2l + 1$, we felt justified in adopting the relativistic Schrödinger equation (5). For small l, the δ_l's were calculated for 40 and 11 kev from the WKB expression (6); for large l (≥ 25), it was found that the δ_l^0's (3) and δ_l's (6) were in excellent agreement, as anticipated from the work of Bartlett and Welton.[6] With the δ_l's obtained in this way (Table I), we have evaluated the magnitudes $|f(\theta)|$ and the arguments $\eta(\theta)$ of the complex scattering amplitudes (Table II). The δ_l's for U can also be computed over the entire l range from the asymptotic expression (15) below. In this case, although the δ_l's differ from the above by as much as 8% at 40 kev and 15% at 11 kev, the resultant magnitudes and arguments in no case

Table I

Selected Values of δ_ℓ

ℓ	Uranium		Fluorine	
	40 kev	11 kev	40 kev	11 kev
0	6.11	7.20	0.571	1.05
2	3.49	4.67	0.414	0.555
4	2.47	2.96	0.317	0.391
6	1.87	2.06	0.258	0.297
8	1.53	1.52	0.218	0.234
10	1.26	1.16	0.189	0.188
15	0.847	0.679	0.135	0.113
20	0.602	0.441	0.101	0.071
25	0.452	0.302	0.077	0.046
30	0.353	0.212	0.059	0.029
35	0.282	0.152	0.046	0.019
40	0.228	0.110	0.036	
50	0.155	0.059	0.022	
70	0.076	0.018		
100	0.028			

Table II

Magnitudes and Arguments of the Scattering Amplitudes

θ	Uranium								Fluorine					
	40 kev				11 kev				40 kev			11 kev		
	$\lvert f(\theta)\rvert$	$\eta(\theta)$	$f^B(\theta)$	$\eta^B(\theta)$	$\lvert f(\theta)\rvert$	$\eta(\theta)$	$f^B(\theta)$	$\eta^B(\theta)$	$\lvert f(\theta)\rvert$	$\eta(\theta)$	$f^B(\theta)$	$\lvert f(\theta)\rvert$	$\eta(\theta)$	$f^B(\theta)$
0	14.51	0.317	17.24	0.50	12.01	0.414	16.36	0.90	2.31	0.079	2.32	2.15	0.141	2.20
1	10.30	0.424	12.78		10.64	0.456	14.88		1.90	0.093	1.91	2.03	0.148	2.08
2	5.54	0.687	7.52		7.85	0.579	11.78		1.24	0.128	1.24	1.73	0.169	1.77
3	3.21	1.00	4.74	1.39	5.37	0.772	8.86	1.51	0.776	0.179	0.781	1.39	0.201	1.43
4	2.08	1.31	3.27		3.67	1.01	6.72		0.507	0.231	0.511	1.08	0.243	1.12
5	1.46	1.60	2.42		2.61	1.28	5.23		0.349	0.281	0.352	0.841	0.290	0.871
6	1.08	1.88	1.87	2.41	1.94	1.57	4.18	2.63	0.252	0.329	0.254	0.660	0.341	0.685
7	0.837	2.16	1.49		1.52	1.85	3.44		0.190	0.376	0.192	0.525	0.396	0.546
8	0.683	2.42	1.21		1.24	2.13	2.88		0.148	0.420	0.149	0.424	0.447	0.442
10	0.500	2.89	0.842	3.44	0.930	2.64	2.12	3.96	0.096	0.487	0.098	0.291	0.552	0.302
12	0.403	3.26	0.624		0.756	3.03	1.63		0.060	0.551	0.070	0.211	0.651	0.218
14	0.330	3.53	0.478		0.623	3.34	1.30		0.051	0.623	0.052	0.162	0.738	0.164
16	0.267	3.74	0.378	4.64	0.520	3.60	1.06	5.60	0.040	0.676	0.041	0.128	0.830	0.128

differ by more than 3% from those in Table II, the relative error increasing with increasing θ.

In the application of these results to the molecule UF_6, the assumption is made that multiple scattering and valence distortion are negligible. Then for visual data the following expression for the intensity function (specialized for the case of UF_6) is suitable:

$$I(s)\,K(s) = (6/r_{U\text{-}F})\cos\left[\eta_U(\theta) - \eta_F(\theta)\right]\sin(r_{U\text{-}F}s) + \left(|f_F(\theta)|/|f_U(\theta)|\right) \tag{9}$$

$$\times\left\{(12/r_{F\text{-}F})\left(\exp\left[-(a_{F\text{-}F}+a_{U\text{-}F})s^2\right]\right)\sin(r_{F\text{-}F}s) + (3/r_{F\text{-}F})\left(\exp\left[-(a_{F\text{-}F}+a_{U\text{-}F})s^2\right]\right)\sin(r_{F\text{-}F}s)\right\},$$

where $I(s)$ is the modified scattering intensity, $K(s)$ is a smoothly decreasing function of s, and $e^{-a_{ij}s^2}$ is the temperature factor for the distance r_{ij} between atoms i and j.[1,10] Using the complex amplitudes obtained above and a symmetric UF_6 model ($r_{U\text{-}F}$ = 2.00 Å, $r_{F\text{-}F}$ = 2.83 Å, and $r_{F\text{-}F}$ = 4.00 Å) with $a_{U\text{-}F} = 1.5\ 10^{-3}$ and $a_{F\text{-}F} = 2.2\ 10^{-3}$,[11] we have evaluated the function $I(s)K(s)$ at 11 and 40 kev. Fig. 1 compares the calculated and the visually estimated versions of this function. When one considers that the visual curves are significant only for comparisons of intensity over a small range of s (e.g., that one usually can compare the height of max n only with the average of the heights of max $n+1$ and max $n-1$), the agreement is excellent. For the present purpose, the most significant parts of the patterns are the very sensitive regions where $\eta_U(\theta) - \eta_F(\theta) = \pi/2$ and these are reproduced satisfactorily (Table III).

Table II also provides a comparison with the magnitudes $f^B(\theta)$ calculated by the first Born approximation[12] (using (18) and (19)) and the phase angles $\eta^B(\theta)$ for U calculated by the second Born approximation.

For the latter it was necessary to extend the calculations of Glauber and Schomaker[2] to the potential for U used here. Their formula is

$$\eta_l^B(\theta) = \eta^B(\bar{k}', \bar{k}) = \frac{k}{4\pi i^l(\theta)} \int f^B(\bar{k}', \bar{k}'') f^B(\bar{k}'', \bar{k}) d\Omega_{\bar{k}''} \qquad (10)$$

where $\bar{k}$ and $\bar{k}'$ refer to the directions of incidence and scattering respectively, and $\bar{k}''$ is integrated over the sphere $|\bar{k}''| = k$. When the potential (7) for U was inserted and the integration performed there resulted

$$\eta^B(\theta) = \frac{a^2}{2kf^B(\theta)\cos(\theta/2)} \sum_{i=1}^{3} \sum_{j=1}^{3} \frac{a_i a_j}{h_{ij}} \left(\tanh^{-1} \frac{h_{ij} \cos(\theta/2)}{\varepsilon_{ij}\varepsilon_{ii} - \cos^2(\theta/2)} + \tanh^{-1} \frac{h_{ij} \cos(\theta/2)}{\varepsilon_{ij}\varepsilon_{jj} - \cos^2(\theta/2)} \right), \qquad (11)$$

$$\varepsilon_{ij} = 1 + (b_i^2 + b_j^2)/4k^2a^2 ,$$

$$h_{ij} = \left[(b_i^2 - b_j^2)^2/(4k^2a^2)^2 - (\varepsilon_{ij}^2 - \cos^2(\theta/2))\tan^2(\theta/2) \right]^{1/2} ,$$

which is in serious disagreement with the partial waves values and with experiment, as may be seen from Tables II and III. The good agreement with experiment obtained previously[2] must be due to a fortuitous cancellation of errors. For heavy atoms the screened-coulomb field is quite unsatisfactory and (10), even at 40 kev, is inadequate.

It is planned to extend the calculations for 40 kev electrons to other atoms with the hope of achieving a sufficiently general theoretical basis for electron diffraction studies of the molecular structures of gases.

We thank Professor Verner Schomaker for reading this paper and for making many helpful suggestions.

Table III

Values of s where $\eta_U(0) - \eta_F(0) = \pi/2$

Voltage, kev	$s_{observed}$	$s_{partial\ waves}$	$s_{2nd\ Born}$
40	10.7 ± 0.6	10.9	7.7
11	6.6 ± 0.6	7.1	3.8

IV. APPENDIX - MATHEMATICAL DETAILS

The Phases δ_ℓ and δ_ℓ^0

When computing δ_ℓ it is convenient to split up (6) as follows:

$$\delta_\ell = \int_{r_1}^{r_3} G(r)\,dr - \int_{r_2}^{r_3} G_0(r)\,dr + \int_{r_2}^{\infty} \left[G(r) - G_0(r)\right] dr = I_1 - I_2 + I_3. \quad (12)$$

Here, r_3 is sufficiently large so that for $r > r_3$, $G(r)$ and $G_0(r)$ do not differ by more than 10%. Then I_3 reduces to

$$I_3 = \frac{km}{2\ell^2} \int_{r_3}^{\infty} \left[V(r)/G_0(r)\right] dr. \quad (13)$$

r_1 was evaluated graphically and I_1 was integrated numerically using Simpson's rule; I_2 can be integrated analytically. I_3 (13) can be expressed in terms of various power expansions and when $V(r)$ is given by (7), the following expression is convenient:

$$I_3 = -\alpha \sum_{i=1}^{3} a_i \int_{r_2}^{\infty} dr\, e^{-b_i r/a} \Big/ \left[r^2 - (\ell + \tfrac{1}{2})^2/k^2 \right]^{1/2}$$

$$= -\alpha \sum_{i=1}^{3} a_i \left\{ K_0(u_i) - e^{-u_i} \left[m - u_i \frac{m^3}{3!} + (3u_i^2 - u_i) \frac{m^5}{5!} - (15u_i^3 + u_i - 15u_i^2) + \ldots \right] \right\} \quad (14)$$

$$u_i = b_i(\ell + \tfrac{1}{2})/km, \quad m = \cosh^{-1}\left(r_3 k/(\ell + \tfrac{1}{2})\right).$$

For large values of ℓ (≥ 25), it was found that $r_1 \simeq r_2 \simeq r_3$, so that (12) reduces to

$$\delta_\ell = -\alpha \sum_{i=1}^{3} a_i K_0(u_i). \quad (15)$$

For the same potential, (3) becomes

$$\delta_\ell^{\,o} = -\alpha \sum_{i=1}^{3} a_i Q_\ell \left(1 + \tfrac{1}{2}\left(\frac{b_i}{ka}\right)^2\right) . \tag{16}$$

The Q_ℓ's were computed for $0 \leq \ell \leq 10$ using the polynomial expansions,[13] for $\ell \geq 10$ they were evaluated using Watson's relation[14]:

$$Q_\ell(\cosh \xi) \sim \exp\left[-(\ell + \tfrac{1}{2})(\xi - \tanh \xi)\right] \operatorname{sech}^{1/2} \xi \; K_0\left[(\ell + \tfrac{1}{2})\tanh \xi\right] + O(e^{-\ell\xi}/\ell). \tag{17}$$

At $\ell = 10$, (17) gave values in excellent agreement with the exact values and therefore its use was justified for higher ℓ. When computing the phases for large ℓ (> 25), only the term for $i = 3$ is of importance in (7). Since the corresponding ξ is much less than unity, (17) reduces very nearly to

$$K_0\left[(\ell + \tfrac{1}{2})\,\xi\right] \approx K_0\left[(\ell + \tfrac{1}{2})\, b_3/ka\right]$$

so that the δ_ℓ's and $\delta_\ell^{\,o}$'s are in close agreement.

Corresponding quantities for the F potential (8) can be readily obtained: Integrals involving a term of the form $cre^{-\beta r}$ are obtained by differentiating with respect to β the integrals already obtained for terms of the form $ce^{-\beta r}$ (the U potential).

The Scattering Amplitudes

In summing (1), the convergence of the real part is improved by subtracting $f^B(\theta)$ as given by its series expansion (2) and adding it as obtained by the integration of (4). The integrated expressions are respectively for U and F

$$f^B(\theta) = -2ka^2 \sum_{i=1}^{3} a_i (b_i^2 + a^2 s^2)^{-1} \tag{18}$$

and

$$f^B(\theta) = -2ka \left[(\beta_1^2 + s^2)^{-1} + (2c\beta_2)(\beta_2^2 + s^2)^{-2} \right] \tag{19}$$

By substituting the following asymptotic expressions[15]

$$K_o(x) \sim (\pi/(2x))^{1/2} e^{-x} \tag{20}$$

and

$$P_\ell(\cos\theta) \sim (\tfrac{\pi}{2} \ell \sin\theta)^{-\frac{1}{2}} \sin\left[(\ell + \tfrac{1}{2})\theta + \tfrac{\pi}{4} \right] \leq (\tfrac{\pi}{2} \ell \sin\theta)^{-\frac{1}{2}} \tag{21}$$

into the respective expressions for the real and the imaginary parts of $\underline{f}(\theta)$, it was shown that negligible errors would arise from termination of the summation at $\underline{\ell} = 70$ for the real part and at $\underline{\ell} = 100$ for the imaginary part, for $\theta \gg 1°$. For $\theta = 0°$, $\underline{P}_{\underline{\ell}}(\cos\theta) = 1$ and an exact termination correction can be made.

The $\underline{P}_{\underline{\ell}}(\cos\theta)$ were obtained from the available tables up to $\underline{\ell} = 10$ and for $10 \leq \underline{\ell} \leq 100$, $1° \leq \theta \leq 16°$, they were computed from the relation

$$P_{\ell}(\cos\theta) \sim (\theta/\sin\theta)^{1/2} J_0\left[(\ell+\tfrac{1}{2})\,\theta\right] \qquad (22)$$

which may be derived from the corresponding asymptotic expressions.[16] Equation (22) was satisfactory for $\underline{\ell}$ as low as 5 over the whole range of θ indicated in Table II.

FOOTNOTES AND REFERENCES

* This work was supported in part by ONR Contract N6-onr-24423.

** National Science Foundation Predoctoral Fellow, 1952-1953.

*** Contribution No. 1812

1. V. Schomaker and R. Glauber, Nature, 170, 290 (1952).

2. R. Glauber and V. Schomaker, Phys. Rev., 89, 667 (1953).

3. Preliminary results by G. Felsenfeld and J. Ibers.

4. As a general reference, we give N. F. Mott and H.S.W. Massey, The Theory of Atomic Collisions (Oxford University Press, London, 1949), second edition, particularly Chapter VII.

5. R. E. Langer, Bull. Am. Math. Soc., 40, 574 (1934); Phys. Rev., 51, 669 (1937).

6. J. H. Bartlett, Jr. and T. A. Welton, Phys. Rev., 59, 281 (1941).

7. G. Molière, Z. Naturforsch., 2a, 142 (1947).

8. F. W. Brown, Phys. Rev., 44, 214 (1933).

9. See Reference 4, Chapter IV, Equation 23.

10. P. Shaffer, Jr., V. Schomaker, and L. Pauling, J. Chem. Phys., 14, 659 (1946).

11. S. H. Bauer, J. Chem. Phys., 18, 27 (1950).

12. It should be noted that $f^B(\theta)$ is related to $F(\theta)$, the x-ray form factor by the relation

$$f^B(\theta) = (-2k\alpha)/(s^2)\left[1 - (F(\theta))/(Z)\right]$$

The $F(\theta)$ for U obtained from the corresponding $f^B(\theta)$ given in Table II agree to within $1\frac{1}{2}\%$ with the Thomas-Fermi values given in Internationale Tabellen zur Bestimmung von Kristallstrukturen (Berlin, 1935), Vol. 2, p. 573. The $F(\theta)$ for F agree to within 10% with those of R. W. James and G. W. Brindley (Phil. Mag., 12, 81 (1931)), and to within 6% with

the $\bar{f}$ of R. McWeeny (Acta Cryst., 4, 513 (1951)); our values being in general lower than those of McWeeny and higher than those of James and Brindley. We suspect these differences arise from differences in the models used.

13. Cayley, Mess. Math., XVII, 21 (1887). The same polynomials with decimal coefficients are given with some errors by N. Rosen, Phys. Rev., 38, 255 (1931).

14. G. N. Watson, Mess. Math., XLVII, 151 (1918).

15. See, for example, E. Jahnke and F. Emde, Funktionentafeln (Dover Publications, New York, 1945), fourth edition, p. 137 noting that

$$K_o(x) = (\pi/2)\, i\, H_o^{(1)}(ix),$$

and p. 117.

16. See Reference 15, pp. 117, 138.

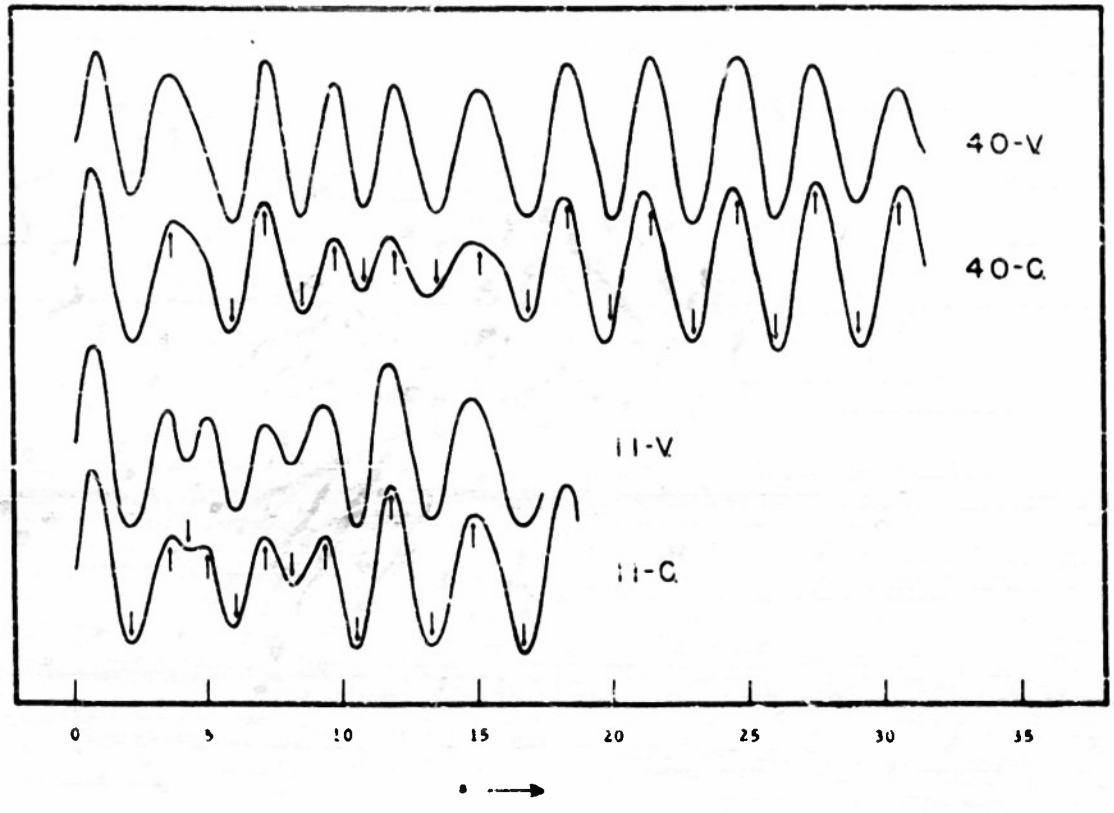

Fig. 1. Intensity curves for UF_6. "V" visual, "C" calculated for "40" or "11" kev. Further photographs will be made both at 40 and 11 kev, and the visual curves (40-V is due to Dr. Otto Bastiansen and 11-V to Felsenfeld and Ibers[3]) are not to be regarded as final.

3. X-ray Crystallographic Studies of Beryllium Boride and the Alleged Copper Boride

From the Thesis of Morton E. Jones, June 1953

a. Beryllium Boride

b. Copper Boride

Beryllium Boride

The formation of boron hydrides by acid hydrolysis of the product of heating magnesium with boric oxide appears to occur in similar yield if beryllium is used in place of the magnesium,[1] so that if the first process involves the magnesium boride MgB_2 described in our Technical Report No. 3 (June 15, 1952), the second might well involve a similar beryllium boride. However, the beryllium atom is so small compared to the other metal atoms of the MB_2 series that the composition BeB_2 is rather unlikely. Accordingly, an attempt to prepare a beryllium boride and study its crystal structure seemed desirable.

Experiments and Results.- A mixture of approximately equal weights of commercial powdered boron (99.05%) and powdered beryllium (premium grade) was heated with a gas-oxygen flame to about 1400° C for several minutes in a beryllium oxide crucible under a current of helium. (Because beryllium is so very toxic, all operations of handling and heating were carefully performed in a hood.) The resulting inhomogeneous mass contained coppery particles, some of which were powdered, sealed in a thin-wall soft glass capillary tube about 1/4 mm in diameter, and photographed with nickel-filtered CuKα radiation in a Straumanis-type camera of nominal radius 18/π cm. The photograph, showing a rather small number of macro-crystalline lines in addition to a complex spectrum of smoother lines, indicated the existence of at least two phases. The macro-crystalline lines correspond to a face-centered cubic unit cell with $a_o \simeq 4.66$ Å and their intensities suggested a fluorite type of structure.

Photographs of further preparations (mostly carried out in a quartz tube rather than the beryllium oxide crucible) indicated maximum yield of the cubic phase for an initial atomic ratio Be:B between 2:1 and 1:1, but closer to 2:1 than 1:1, and showed that the other lines were probably due to one or more phases with higher beryllium content. Attempts to prepare the cubic phase in pure form for reliable determinations of composition and density were unsuccessful. The positions and intensities of the cubic lines were measured on several of the photographs by the methods described for magnesium boride. Least squares refinement on the $\sin^2\theta_{hk\ell}$ values then led to the result $a_o = 4.6583 \pm 0.0017$ Å; the observed and calculated values of $\sin^2\theta_{hk\ell}$ are given in Table I.

Structure factors were calculated for a structure with 8 Be at (1/4,1/4,1/4;3/4,3/4,3/4) + F.C. and 4 B at 0,0,0 + F.C (the fluorite positions) using the atomic form factors of James and Brindley.[2] The resulting moduli showed approximate agreement with the observed intensities, and the signs, together with the observed moduli $|F_{obs.}|$, led to the plot of $\rho(x,x,x)$ vs x shown in Figure 1. In addition to the expected peaks at 0,0,0 and 1/4,1/4,1/4, there is a peak at 1/2,1/2,1/2 about one-quarter as high as the main peaks. This position has eight beryllium neighbors at a distance of 2.02 Å--less, even, than the Be-Be single bond distance of 2.14 Å--and cannot contain a beryllium atom. It therefore appears that, in addition to eight beryllium atoms and four boron atoms, the unit cell contains approximately one other boron atom randomly distributed among the four positions 1/2,1/2,1/2 + F.C., giving a composition approximating Be_8B_5. The structure

Table I

hkl	$\sin^2\theta^{obs.}_{hkl}$	$\sin^2\theta^{calc.}_{hkl}$	$F^{2\,obs.}_{hkl}$	$F^{2\,calc.}_{hkl}$
111	0.0822	0.0822	100	57.2
200	.1094	.1095	10	11.6
220	.2192	.2191	542	534
311	.3003	.3012	26	28.5
222	.3269	.3286	4	18.4
400	.4372	.4382	374	426
331	.5201	.5203	27	21.6
420	.5474	.5477	7	15.6
422	.6572	.6473	405	332
(333) ( ) (511)	.7392	.7394	31	18.7
440	.8765	.8764	235	274
531	.9586	.9585	18	17.1

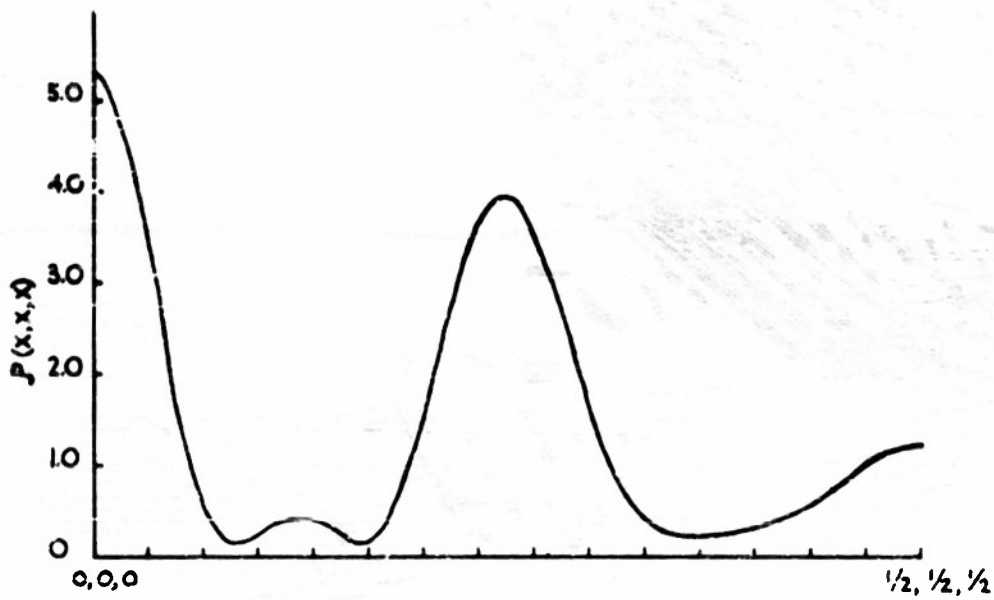

Fig. 1 Electron density along the body diagonal of the beryllium boride unit cell.

factors calculated for this composition are shown with the observed values in Table I; the reliability factor, $R = \sum \left| F^2_{calc.} - F^2_{obs.} \right| / \sum \left| F^2_{obs.} \right|$, is 0.15.

The density and chemical composition are consistent with this structure, if allowance is made for the presence of other phases, but accordingly do not provide any conclusive evidence on the Be_8B_5 phase. The densities of several of the coppery particles, measured by flotation, ranged from 1.96 to 2.20 g./cc.; the calculated density for five boron and eight beryllium atoms in the unit cell is 2.071 g./cc. A chemical analysis was made of an 81.2 mg. sample of the coppery material as dissolved in concentrated HCl. Beryllium was first precipitated with ammonium hydroxide, filtered off with Whatman No. 40 paper, ignited to constant weight, and determined as the oxide. Then, sodium hydroxide was added to the filtrate, the ammonia expelled by boiling, bromine added, and the solution boiled again to insure conversion of all the boron to borate. The pH was adjusted to correspond with a comparison solution containing an approximately equivalent amount of boric acid; methyl red was used as the indicator. Mannitol was added and the solution was titrated with standard 0.1 N sodium hydroxide to a phenolphthalein end point. The result of the analysis was

Be = 70.5 atom %

B = 22.2 atom %

The remaining 7.3% was insoluble in the concentrated HCl, and was doubtless boron in some form; the sample therefore probably contained 29.5 atom % B altogether, as compared to 61.5 atom % beryllium and 38.5 atom % boron for Be_8B_5. Since the powder photographs indicate

that other phases may comprise as much as 30% of the coppery material, and that these phases are on the high beryllium side of Be_8B_5, the results of the analysis are not unreasonable. Direct determination of the exact composition will require a sample of much higher purity than we have so far been able to obtain; and Professor Pol Duwez has kindly consented to investigate the possibility of obtaining improved samples at the Jet Propulsion Laboratory.

Discussion. - The tentative structure, of approximate composition Be_8B_5, is truly an interesting and surprising one. The following remarks may help to lend it credibility.

Of the many metallic borides which have been studied, the great majority contain boron frameworks of some sort, such as chains, hexagonal nets, or three dimensional networks of joined octahedra. The boron-boron bonds in these borides have lengths in the range 1.7-1.8 Å, and would appear to be strong compared to the boron-metal and metal-metal bonds. Moreover, a given structure type is stable over a rather wide range of different metal atoms, as for example in the MB_2 series. Presumably, it is the ability of boron to form the frameworks in these compounds which is chiefly responsible for their formation and stability.

Beryllium carbide, Be_2C, has been studied[3] and found to have the fluorite structure. We may, therefore, consider the structure of Be_8B_5 to be a compromise between a tendency for beryllium to adopt the fluorite arrangement in these structures and the tendency for boron to form some sort of network containing boron-boron bonds. This, boron does in the proposed Be_8B_5 structure, but not in the related ideal fluorite arrangement.

Also, it must be noted, Be_8B_5, in contrast to Be_8B_4, has almost identically the same number of valence electrons per unit cell as Be_8C_4, and this may be significant.

Copper Boride

Our work on magnesium boride led also to an interest in Marsden's report of a copper boride Cu_3B_2.[4] Marsden heated a mixture of amorphous boron and metallic copper in a porcelain crucible for 3 - 4 hours to a temperature above the melting point of copper. The brittle, yellowish product resembled iron pyrites in appearance, and, by qualitative analysis, contained copper, silicon, and boron; the density was 8.116 g/cc. Quantitative analysis for copper and silicon, together with the assumption that the sample was a mixture of silica and a copper boride, then led to the formula Cu_3B_2.

Our attempt to prepare this boride was carried out in a similar manner, a current of helium being passed over the sample during the heating period. In addition to unreacted copper and boron, the product contained small particles of a brittle, silvery substance, of density about 8 g./cc.

X-ray powder photographs, prepared from a crushed sample of the substance, turned out to be identical with photographs obtained later from a sample of the copper silicide Cu_3Si. It was noticed that on standing in air fragments of the substance changed until they had the appearance of pyrite. The powder, when heated to 100° C for a short time in the presence of air, also developed this yellow color.

The X-ray photographs and the similarities in preparation and properties of our sample to Marsden's Cu_3B_2, together with the failure of other attempts to prepare a copper boride,[5,6] seem to indicate

that both preparations are actually copper silicide, possibly containing a small amount of boron. The source of silicon in the preparations is without doubt the porcelain crucible.

Additional attempts using the electric arc furnace of the Jet Propulsion Laboratory were unsuccessful, and it seems that no copper boride can be formed by a direct union of the two elements.

References

1. A. Stock, Hydrides of Boron and Silicon, Cornell University Press (1933), Chap. 25.
2. R. W. James and G. W. Brindley, Internationale Tabellen zur Bestimmung von Kristallstrukturen, Gerbruder Borntraeger, Berlin (1935), vol. II, p. 571.
3. M. v.Stackelberg, Z. physik. Chem. (1934), 27B, 53.
4. R. S. Marsden, J. Chem. Soc. (1880), 37, 672.
5. S. A. Tucker and H. R. Moody, J. Chem. Soc. (1902), 81, 14.
6. H. Giebelhausen, Z. anorg. Chem. (1915), 91, 251.